OPEN

Temporal stability of fMRI in medetomidine-anesthetized rats

Nikoloz Sirmpilatze[1,2,3,4*], Jürgen Baudewig[1] & Susann Boretius [1,2,3,4*]

Medetomidine has become a popular choice for anesthetizing rats during long-lasting sessions of blood-oxygen-level dependent (BOLD) functional magnetic resonance imaging (fMRI). Despite this, it has not yet been thoroughly established how commonly reported fMRI readouts evolve over several hours of medetomidine anesthesia and how they are affected by the precise timing, dose, and route of administration. We used four different protocols of medetomidine administration to anesthetize rats for up to six hours and repeatedly evaluated somatosensory stimulus-evoked BOLD responses and resting state functional connectivity. We found that the temporal evolution of fMRI readouts strongly depended on the method of administration. Intravenous administration of a medetomidine bolus (0.05 mg/kg), combined with a subsequent continuous infusion (0.1 mg/kg/h), led to temporally stable measures of stimulus-evoked activity and functional connectivity throughout the anesthesia. Deviating from the above protocol—by omitting the bolus, lowering the medetomidine dose, or using the subcutaneous route—compromised the stability of these measures in the initial two-hour period. We conclude that both an appropriate protocol of medetomidine administration and a suitable timing of fMRI experiments are crucial for obtaining consistent results. These factors should be considered for the design and interpretation of future rat fMRI studies.

Functional magnetic resonance imaging (fMRI), relying on blood-oxygen-level dependent (BOLD) contrast[1], is being widely used for the non-invasive mapping of human brain function. Classically, fMRI has focused on the brain's response to a task or stimulus, but more recent task-free (resting state fMRI) approaches have explored spontaneous low frequency fluctuations in the BOLD signal[2,3], and their role in the functional connectivity of healthy and diseased brains[4]. Since the advent of dedicated high-field MR systems, fMRI applications have expanded to experimental animals, especially rodents[5]. This is a promising development for translational preclinical research, since the same technique can be applied to both human patients and animal models. Additionally, the expanding capacity of small animal fMRI to be combined with genetic, pharmacological and surgical manipulations, as well as with electrophysiological and optical recordings, allows the exploration of increasingly complex neuroscientific questions[6–9].

Nevertheless, small animal fMRI poses a methodological challenge: it necessitates the subject's immobility for long imaging times. Animals can be restrained and habituated to head fixation and MR scanner noise, but this is laborious for the researcher, and often stressful for the animal[10–12]. Thus, ethical and practical considerations mandate the use of anesthesia in the majority of small animal fMRI studies. Unfortunately, anesthetics confound fMRI measurements in multiple ways: they may alter neural activity, affect systemic cardiorespiratory physiology, and interfere with cerebral vasculature and neurovascular coupling—the very mechanism giving rise to the BOLD contrast[13,14]. Therefore, there is a need for an anesthetic protocol that ideally provides sufficient, long-lasting sedation, while maintaining neural activity and neurovascular coupling. In pursuit of the above properties, researchers have tried multiple anesthetic agents, including α-chloralose, medetomidine, isoflurane, propofol, urethane, and ketamine-xylazine. These agents have varying effects on the neurovascular system, with each of them presenting a unique set of benefits and drawbacks for fMRI applications[12–18]. This has led to a substantial diversity in anesthetic protocols used for rodent fMRI, compromising the comparability and reproducibility of results.

Of the above anesthetics, the sedative agent medetomidine—a highly selective α_2-adrenergic agonist—holds perhaps the most promise for becoming a routine choice for fMRI applications in rats. Medetomidine comes as an equal mixture of two enantiomers, with the dextro-isomer, dexmedetomidine, being the active component[19,20]. Dexmedetomidine decreases the activity of noradrenergic neurons in the locus coeruleus, producing a state that

[1]Functional Imaging Laboratory, German Primate Center - Leibniz Institute for Primate Research, Göttingen, Germany. [2]Georg-August University of Göttingen, Göttingen, Germany. [3]International Max Planck Research School for Neurosciences, Göttingen, Germany. [4]DFG Research Center for Nanoscale Microscopy and Molecular Physiology of the Brain (CNMPB), Göttingen, Germany. *email: NSirmpilatze@dpz.eu; SBoretius@dpz.eu

	Name	Route	Bolus	Bolus dose (mg/kg)	Infusion rate (mg/kg/h)
1	SC with bolus	SC	yes	0.05	0.1
2	IV with bolus	IV	yes	0.05	0.1
3	IV no bolus	IV	no	—	0.1
4	IV lower dose	IV	yes	0.035	0.07

Table 1. Medetomidine administration protocols used in this study. SC: subcutaneous; IV: intravenous.

mimics non-REM sleep[21]. Conveniently, the drug's effects are reversible by a specific α_2-adrenergic antagonist—atipamezole[19,20]. A protocol based on the continuous infusion of medetomidine, first introduced by Weber *et al.*[22], presents several advantages for fMRI studies: it sedates rats for several hours, leads to robust stimulus-evoked BOLD responses, allows for easy subcutaneous (SC) administration, avoids the need for intubation, and can be used for longitudinal studies with multiple fMRI sessions[23]. Other research groups have since confirmed the benefits of medetomidine infusion and expanded its usage to resting state fMRI[24–27]. Medetomidine anesthesia is currently an established practice for rat fMRI, with at least 40 published articles reporting the use of the original medetomidine protocol, or variations of it (Supplementary Table S1). Its use is expected to rise, owing to the practical advantages and to the increasing availability of techniques that can be combined with rat fMRI.

However, there are several concerns revolving around the duration and stability of medetomidine anesthesia. Medetomidine administration is always preceded by an inhalable gas anesthetic, usually isoflurane, which is used for anesthesia induction and animal preparation. Isoflurane alters brain metabolism[28], strongly suppresses stimulus-evoked hemodynamic responses[29–31], and may introduce widespread correlations in functional connectivity metrics[12,27,32]. The possibility of these effects lingering long after isoflurane discontinuation cannot be excluded[33]. Then there is the issue of medetomidine itself, which is usually given in two steps: first as a bolus loading dose and then as a continuous infusion. The drug exerts strong effects on cardio-respiratory physiology, including severe bradycardia, peripheral vasoconstriction, transient hypertension, hypoxia and hypocapnia[20,23]. Since these parameters are expected to influence the BOLD mechanism, time-varying effects on physiology could translate into unstable BOLD-based readouts. Another important concern is the restricted duration of anesthesia, with animals reported to spontaneously wake up despite the continuous infusion of medetomidine. Tolerance to the drug's sedative effects has been blamed for this, with researchers proposing to counter it by stepping up the infusion rate[25]. All the above issues are further compounded by the lack of consensus regarding the exact administration scheme; protocols vary in administration route and dose, while some researchers choose to omit the bolus (see Supplementary Table S1).

These concerns imply that commonly reported fMRI readouts, namely stimulus-evoked BOLD responses and resting state functional connectivity (RSFC), might not be stable over long-lasting imaging sessions. It is unclear when a steady state is reached by these readouts, for how long it is maintained, and how it is affected by various medetomidine administration choices. An answer to these questions would enable researchers to design rat fMRI experiments in a way that maximizes the duration of the steady state. This would increase the available experimental time, decrease variance, and ultimately reduce the total number of required animals, all the while promoting comparability among studies.

To achieve the above goals, we examined how stimulus-evoked BOLD responses and RSFC evolve over time during medetomidine anesthesia. We tested four different protocols for medetomidine administration (Table 1, Fig. 1a) on two separate sessions: first on a laboratory bench and then inside a small animal MR-system. During the latter session, we performed multiple repeated fMRI measurements (runs), with consecutive runs being alternated between somatosensory stimulus-evoked fMRI with electrical forepaw stimulation (EFS-fMRI) and resting state fMRI (RS-fMRI) (see Fig. 1b,c). The acquired runs, 283 EFS-fMRI and 295 RS-fMRI in total, spanned a period of 0.5–6 hours relative to the start of medetomidine administration. For each medetomidine protocol, we report the achieved duration of anesthesia and the following measures across time: heart and respiratory rates (HR and RR); localization and amplitude of stimulus-evoked responses; strength and structure of RSFC. Based on our findings, we make recommendations regarding the administration protocol of medetomidine and the timing of fMRI experiments within the protocol.

Results

Anesthesia duration and physiology. Out of all 48 anesthesia sessions, 27 lasted for the full six hours, while 21 ended with a spontaneous wake-up (spontaneous movement for bench sessions; rapid rise in RR for fMRI sessions). These wake-up incidents occurred across session types (8/24 bench; 13/24 fMRI) and medetomidine protocols (4, 6, 7, and 4 out of 12, for protocols 1–4 respectively). However, only a few of those occurred early, with 35/48 sessions (72.9%) exceeding five hours in duration (Fig. 2a). The HR and RR followed similar temporal trends across all four medetomidine protocols (Fig. 2b). HR decreased rapidly after the introduction of medetomidine, dropping by approximately 50% within the first hour of anesthesia. After that it showed only a slight tendency to gradually recover over time. The RR also underwent rapid changes in the first hour: it started at 40–70 bpm under isoflurane, decreased in response to medetomidine introduction, and gradually recovered following the discontinuation of isoflurane. As was the case with HR, it remained mostly stable after the first hour. HR and RR traces for individual anesthesia sessions can be found in Supplementary Figs S3 and S4 respectively.

Areas activated by the stimulus. For each EFS-fMRI run we identified the active areas using a first-level general linear model analysis. The thresholded statistical maps (cluster threshold, z > 3.1, p = 0.05) were binarized
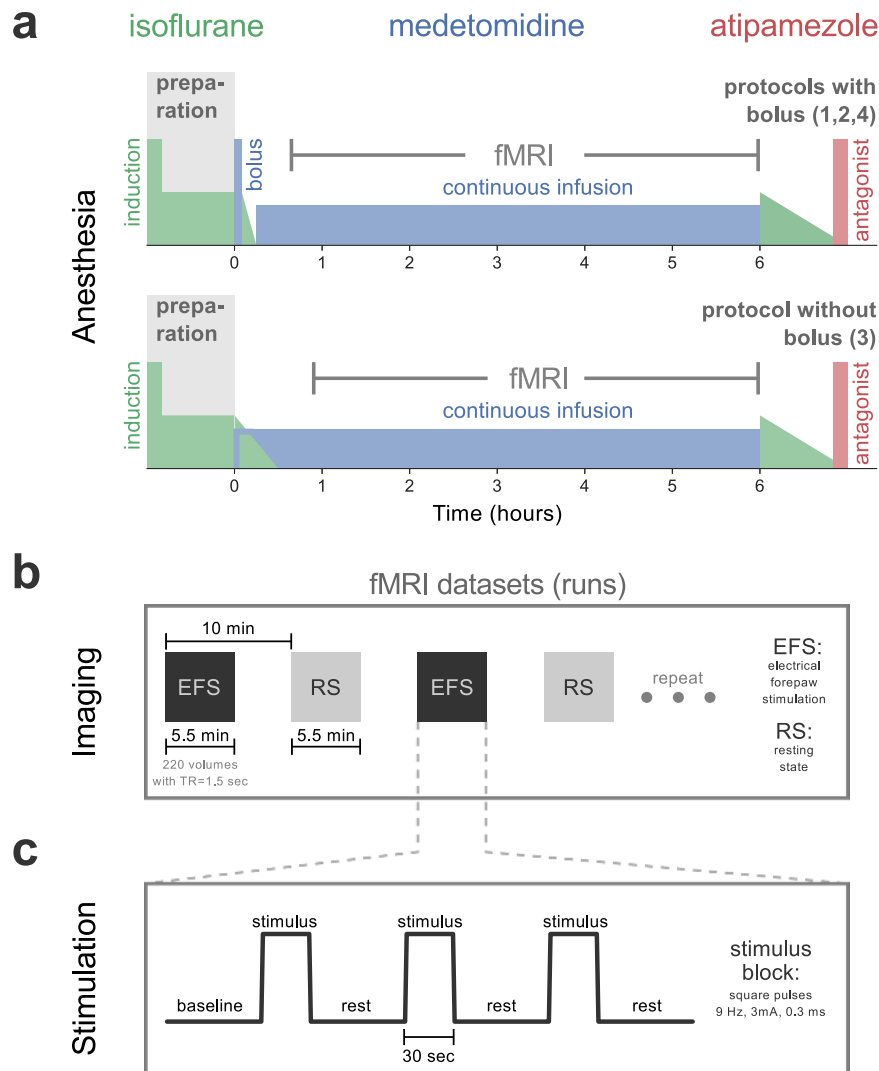
Figure 1. Anesthetic protocols and fMRI acquisition. **(a)** The general outline of the applied anesthetic protocols. For all four protocols (see Table 1), isoflurane was used to induce unconsciousness (5%) and during animal preparation (2–3%). For protocols 1, 2, and 4, a bolus of medetomidine was given after the preparation phase, followed by a gradual reduction of isoflurane and its eventual discontinuation 10 min later; continuous infusion of medetomidine commenced 15 min after the bolus. The bolus was omitted for protocol 3, with continuous infusion starting directly after preparation, and isoflurane being gradually reduced to zero over the course of 20–25 min. Anesthesia was maintained for a maximum of six hours since the start of medetomidine administration (time = 0). In the end, animals were provided with 2% isoflurane and freed from all equipment. Atipamezole was injected SC to antagonize medetomidine effects and to facilitate a smooth recovery. **(b)** Multiple fMRI runs were acquired per anesthesia session, with consecutive runs being alternated between somatosensory fMRI with electrical forepaw stimulation (EFS-fMRI) and resting state fMRI (RS-fMRI) with no stimulus. The stimulation paradigm applied during EFS-fMRI runs is shown in **(c)**.

(1 for active voxels, 0 elsewhere) and averaged across all EFS-fMRI runs to produce an activation probability map. The probability map revealed a consistently active cluster, anatomically corresponding to the left (contralateral to the stimulus) forelimb region of the primary somatosensory cortex—abbreviated as S1FL (Fig. 3a1). This cluster's center was active in 85.16% of all EFS-fMRI runs, whereas no other area was active in more than 7% of runs. To ensure that there was no systematic shift in the location of the active S1FL cluster, the 283 first-level activation maps were split into 12 groups according to the applied medetomidine protocol and the time-window since the start of medetomidine administration (early: 0–2 h; middle: 2–4 h; late: 4–6 h). Examination of activation probability maps from all groups (Fig. 3a2) verified that the active cluster's location remained stable across time and medetomidine protocols.

Shape and strength of stimulus-evoked responses. The portion of the S1FL that was significantly active in at least 30% of all 283 EFS-fMRI runs was taken as a functionally-defined region-of-interest (ROI). For each EFS-fMRI run, this ROI's mean BOLD time course was extracted, normalized to the pre-stimulus baseline,
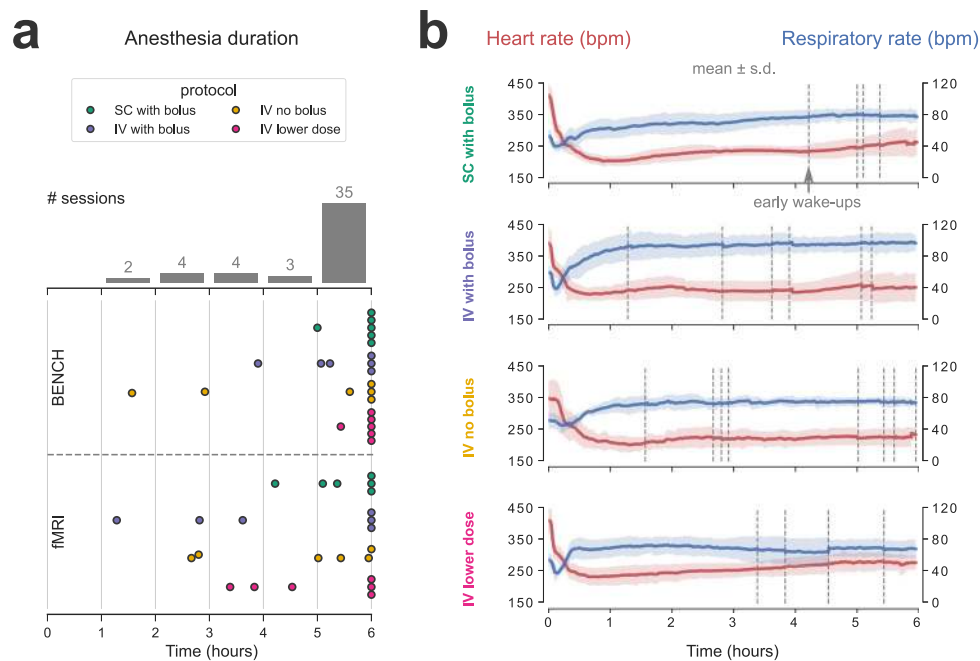
Figure 2. Anesthesia duration and physiology. **(a)** Anesthesia duration is plotted (dots) separately for bench and fMRI sessions, across all four medetomidine protocols. The bars represent a histogram of anesthesia durations, with all 48 anesthesia sessions binned into one-hour intervals. **(b)** Heart and respiratory rates (in beats/breaths per minute—bpm), pooled from both bench and fMRI sessions of each medetomidine protocol, are plotted as an across-session mean (solid line) ± s.d. (shaded area). Each of the four medetomidine protocol groups consists of twelve sessions—six animals with two sessions each. The time-points of early wake-ups are indicated with vertical dashed lines. Heart and respiratory rate traces for individual sessions can be found in Supplementary Figs S3 and S4 respectively.

and averaged across stimulation blocks to produce an event-related average. This was used to extract the peak % signal change (peak ΔBOLD), as a measure of stimulus-evoked BOLD response strength (Fig. 3b). The examination of event-related averages revealed that the shape of S1FL BOLD responses was very similar across the four medetomidine protocols (Fig. 3c). The signal exhibited a sharp peak about 3 s after stimulus onset, followed by a plateau lasting till the end of the 30 s stimulation.

We tested the dependence of peak ΔBOLD on time (early, middle and late two-hour-long time-windows), medetomidine protocol, and their interaction. The medetomidine protocol alone had no effect (ANOVA: F = 1.01, p = 0.38), but we found a strong time dependence (F = 37.65, p < 0.001) and a significant interaction between medetomidine protocol and time-window (F = 4.35, p < 0.001). Post-hoc pair-wise t-tests with p-value adjustment for multiple comparisons (Holm method) revealed varying temporal trends depending on the medetomidine protocol (Fig. 4a,b). Protocol 2 (IV with bolus) led to temporally stable BOLD responses (mean peak ΔBOLD of about 2.3% across time-windows), while the other three protocols led to a significant decrease in response strength between the early and the middle time-windows. Despite their differing temporal trends, all four protocols converged to a mean peak ΔBOLD of 2–3% after the initial two hours of medetomidine anesthesia (Fig. 4c). The results of all statistical comparisons can be found in Supplementary Tables S9–S11.

Resting state functional connectivity. RSFC was probed by examining the pair-wise correlations between the BOLD time courses of 28 anatomically defined ROIs (Fig. 5a). Examination of the pair-wise correlation matrices (Fig. 5b1), and of their network representations (Fig. 5c), showed that the hierarchical structure of the network, i.e. the strength of individual connections relative to each other, was consistent over time for all medetomidine protocols. The network's global RSFC—the mean correlation (Fisher's Z-score) across all unique ROI pairs—was computed for all RS-fMRI runs, and tested for its dependence on time (early, middle and late time-windows), medetomidine protocol, and their interaction. All three factors were found to have a significant effect on global RSFC, according to the results of ANOVA (medetomidine protocol: F = 7.24, p = 0.001; time-window: F = 5.15, p = 0.006; protocol-time interaction: F = 3.41, p = 0.003). Post-hoc pair-wise t-tests followed with p-value adjustment for multiple comparisons (Holm method). Bolus-based medetomidine administration (protocols 1, 2 and 4) was found to sustain stable global RSFC throughout the three time-windows. Omitting the bolus (protocol 3, IV no bolus) led to global RSFC values that were stronger in the early period (p = 0.002 compared to protocol 2; p < 0.001 compared to protocol 4) but decreased significantly between the early and the middle time-windows (p = 0.017). The results of all statistical comparisons can be found in Supplementary Tables S9,S10,S12.
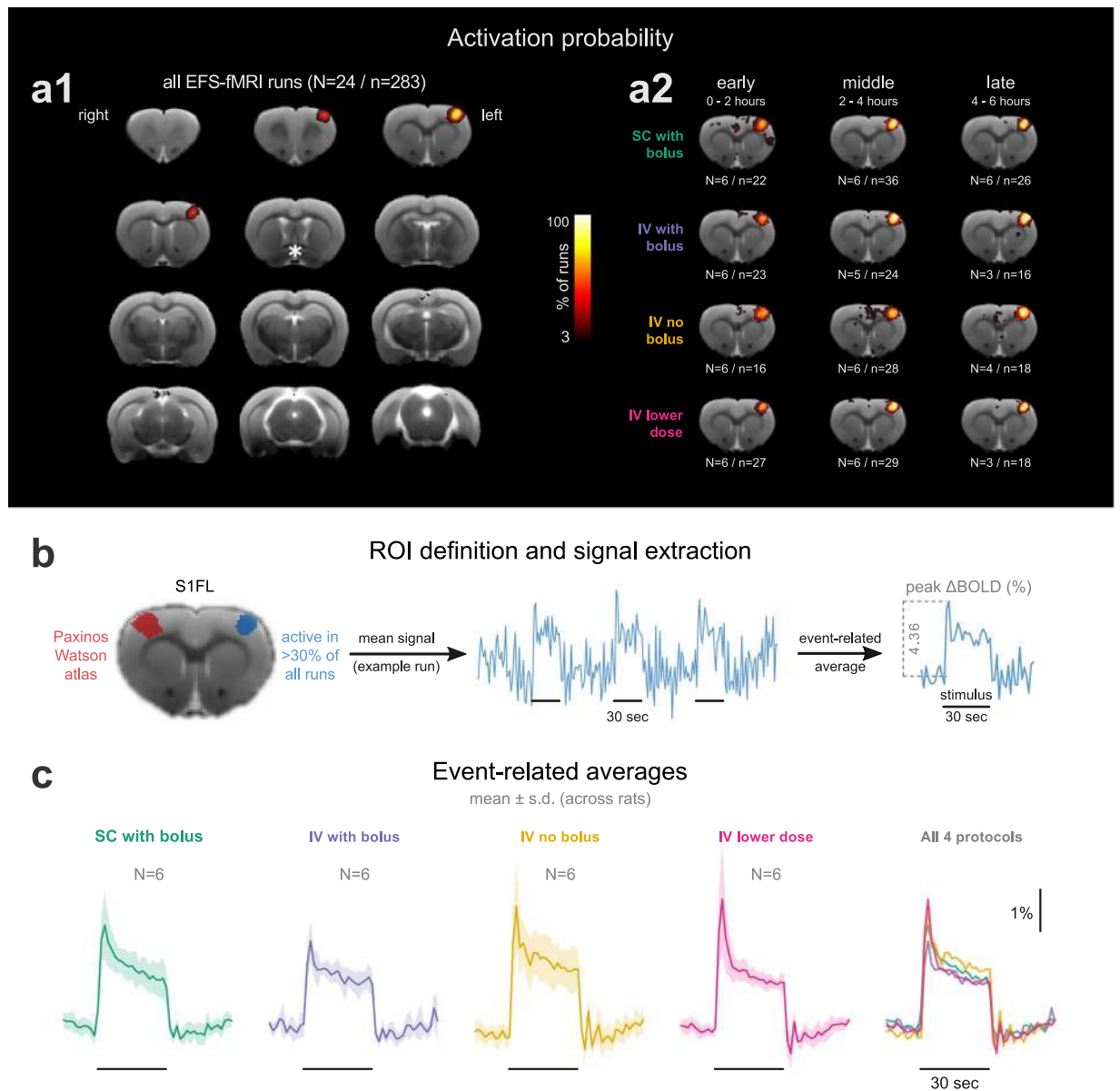
Figure 3. Areas activated by electrical forepaw stimulation (EFS). **(a1)** An activation probability map produced by pooling significantly active clusters from first-level analyses of 283 EFS-fMRI runs. The asterisk marks the crossing of the anterior commissure (AC, −0.36 mm relative to the bregma, according to the Paxinos-Watson rat brain atlas). The rest of the slices are taken at 1 mm intervals from the AC slice. In **(a2)**, the EFS-fMRI runs are grouped according to the applied medetomidine protocol and to the time-window since the start of medetomidine administration (early: 0–2 h; middle: 2–4 h; late: 4–6 h), to produce separate activation probability maps for each group. Only the slice containing the peak activation, 2 mm rostral to AC, is shown for each group. All maps in **(a1,a2)** are thresholded at 3% and overlaid on a T2-weighted structural study template. **(b)** The only consistently active cluster across all runs corresponds to the forelimb region of the left primary somatosensory cortex (S1FL). The location of this cluster is shown alongside the anatomical delineation of the same area from the Paxinos-Watson rat brain atlas. The functionally defined S1FL (area active in >30% of all EFS-fMRI runs) is set as a region-of-interest (ROI) for the extraction of BOLD signal time courses. Such a time course is shown for one example EFS-fMRI run, with the stimulation blocks marked by horizontal lines. Averaging the three stimulation blocks results in an event-related average, from which the peak % signal change (peak ΔBOLD) can be extracted. Event-related average responses (mean ± s.d. across rats) are plotted for all four medetomidine protocols **(c)**. N: number of rats; n: number of fMRI runs.

Discussion

In the present study we evaluated the capacity of medetomidine—administered through four different protocols—to anesthetize rats for up to six hours and sustain temporally stable fMRI measures of stimulus-evoked activity and functional connectivity. We found that anesthesia duration exceeded five hours in most sessions
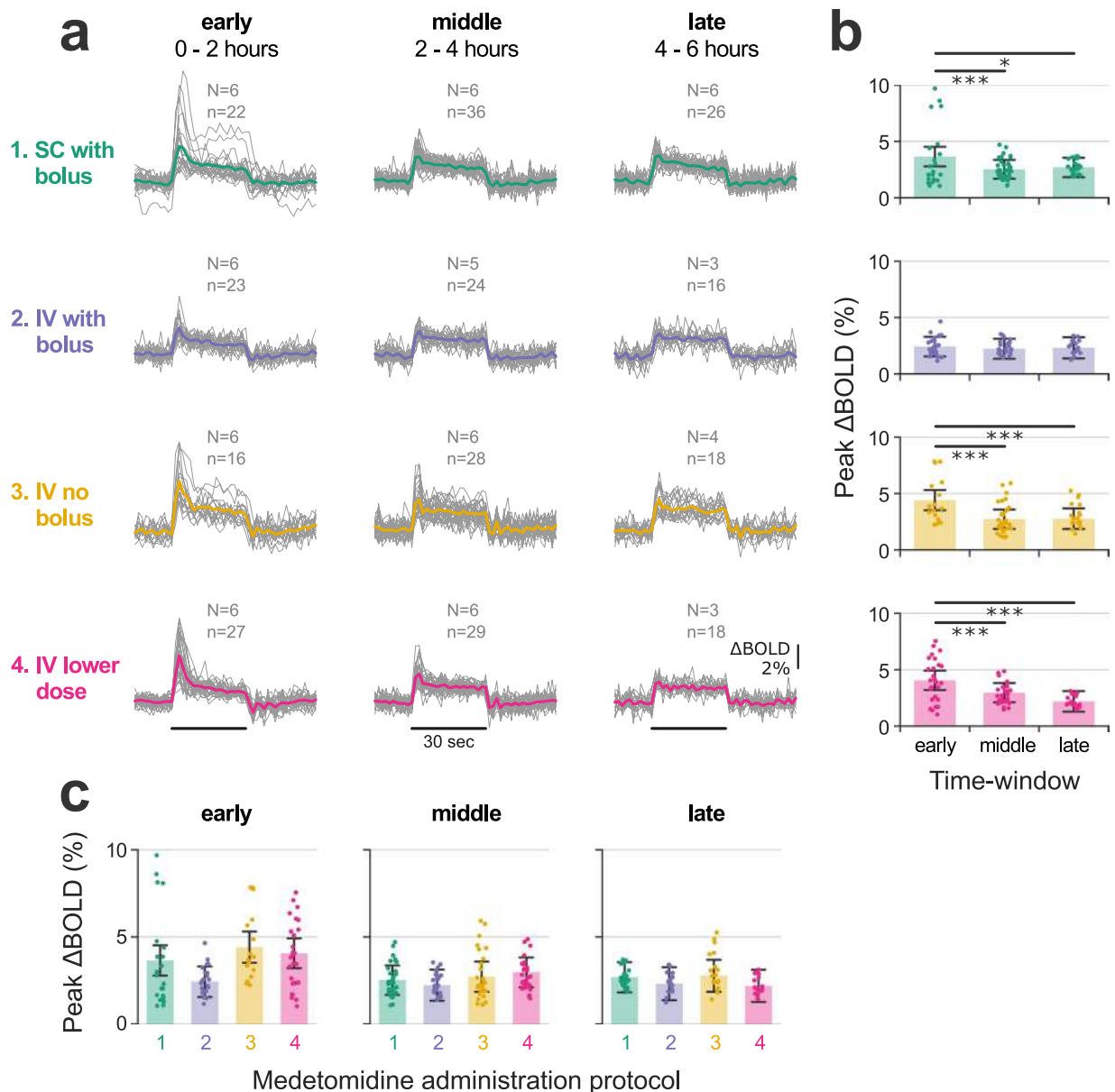
Figure 4. Temporal stability of stimulus-evoked responses. **(a)** Event-related averages produced by averaging the three electrical forepaw stimulation (EFS) blocks of each fMRI run. Single run traces are grouped according to the applied medetomidine protocol and the time-window since the start of medetomidine administration (early: 0–2 h; middle: 2–4 h; late: 4–6 h); each group's mean event-related average is plotted as a thicker trace; EFS duration is represented by horizontal lines. N: number of rats; n: number of fMRI runs. The peak stimulus-evoked signal change (peak ΔBOLD) is extracted from the event-related averages and plotted in **(b,c)**: in **(b)** peak ΔBOLD values are plotted across time-windows for each of the medetomidine protocols, while in **(c)** they are plotted across medetomidine protocols for each of the time-windows. Dots represent single run values, bars show the estimated Least Squares Means, while error margins correspond to the estimated 95% confidence intervals. Asterisks indicate the significance of pair-wise t-tests, after adjusting for multiple comparisons ($p < 0.05$: *, $p < 0.01$: **, $p < 0.001$: ***). Peak ΔBOLD time courses for individual rats are provided in Supplementary Fig. S7a. A complete list of Least Square Means, confidence intervals and pair-wise comparisons can be found in Supplementary Tables S10 and S11.

(35/48 or 72.9%; Fig. 2a), heart and respiratory rates were mostly stable after the first hour of anesthesia (Fig. 2b), and the majority of performed EFS-fMRI runs (241/283 or 85.16%) led to a significant and selective activation of the expected cortical area (Fig. 3a). However, both stimulus-evoked activity and functional connectivity exhibited varying temporal trends depending on the protocol of medetomidine administration (Figs 4 and 5).

Limited anesthesia duration has been referred to as a drawback of medetomidine protocols[34], even though the exact duration is not reported in most papers. According to a study that has addressed this issue, rats anesthetized by constant IV infusion woke up spontaneously 3.5–4 hours into the experiment[25]. However, the rats in that study
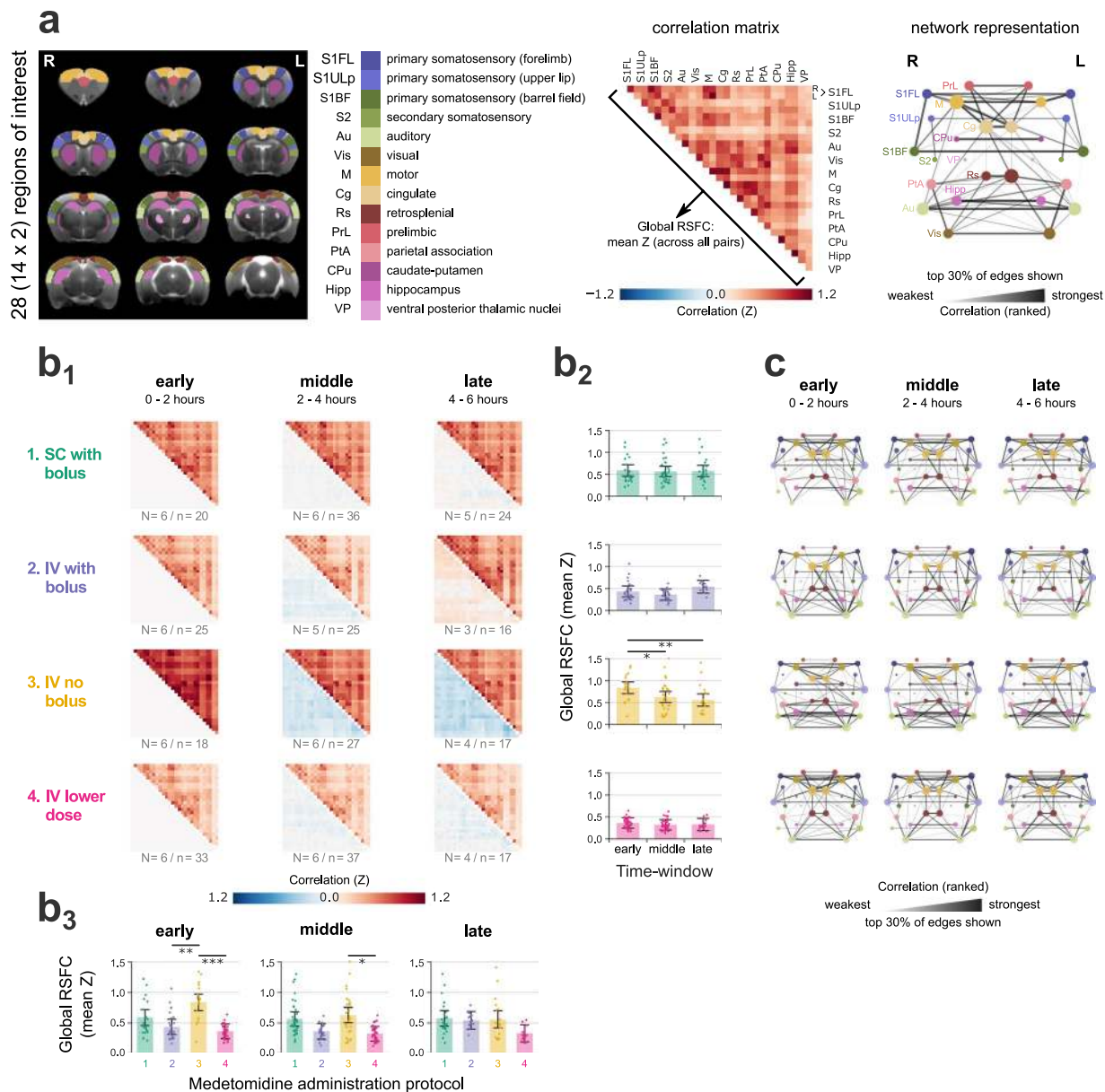
Figure 5. Resting state functional connectivity (RSFC). **(a)** To calculate pair-wise RSFC, 28 regions-of-interest (ROIs) were defined based on the Paxinos-Watson rat brain atlas—14 on each hemisphere. Pearson's correlations were calculated between the BOLD time courses of all unique ROI pairs and transformed into Fisher's Z-scores. A pair-wise correlation matrix is shown for one example RS-fMRI run; the mean correlation (Z-score) across all ROI pairs constitutes the global RSFC. The matrix is also represented as a weighted network graph, with the ROIs as nodes and their pairs as edges. For visualization clarity, only the strongest 30% of edges are shown; edge thickness and opacity scale linearly with the relative rank of the correlation value (the highest Z-score corresponds to the thickest edge); node radius scales with the weighted degree (weighted sum of edges passing through the node). **(b)** The 295 RS-fMRI runs are split into twelve groups according to the applied medetomidine protocol and the time-window since the start of medetomidine administration (early: 0–2h; middle: 2–4h; late: 4–6h). **(b1)** For each group, the upper triangular matrix represents the mean (across runs) pair-wise correlation, while the lower triangular matrix shows the change in correlation compared to each protocol's early period. N: number of rats; n: number of fMRI runs. In **(b2)** global RSFC values are plotted across time-windows for each of the medetomidine protocols, while in **(b3)** they are plotted across medetomidine protocols for each of the time-windows. Dots represent single run values, bars show the estimated Least Squares Means, while error margins correspond to the estimated 95% confidence intervals. Asterisks indicate the significance of pair-wise t-tests, after adjusting for multiple comparisons (p < 0.05: *, p < 0.01: **, p < 0.001: ***). Global RSFC time courses for individual rats are provided in Supplementary Fig. S7b. A complete list of Least Square Means, confidence intervals and pair-wise comparisons can be found in Supplementary Tables S10 and S12. **(c)** The mean correlation matrices (upper triangles of **(b1)**) are also visualized as network graphs, similarly to the example graph in **(a)**.

were tracheotomized and mechanically ventilated, while most rat fMRI experiments—including ours—are conducted in freely breathing animals. The anesthesia durations achieved in our experiments should satisfy the needs of most researchers. That said, the risk of spontaneous wake-ups must be taken into consideration. In our study, these wake-ups occurred more often in fMRI than in bench sessions (13/24 versus 8/24)—a possible effect of the scanner's acoustic noise—and were typically preceded by an increase in RR and arrhythmic breathing. A timely identification of such an RR increase allows the researcher to promptly supply isoflurane through the mask in order to mitigate an un-controlled wake-up, and the associated animal stress. If early wake-ups must be avoided altogether, other administration practices may be warranted, such as stepping up the infusion rate[25], or adding a constant low dose of isoflurane throughout the imaging session[35]. The latter strategy has gained popularity in recent years, on the basis that it provides near-normal physiological conditions[35] and protects against epileptic seizures—which have been reported in animals with medetomidine-only anesthesia[36]. However, this might require mechanical ventilation, since even low doses of isoflurane, when combined with medetomidine, have been shown to suppress the amplitude of stimulus-evoked BOLD responses in spontaneously breathing rats[37].

The recorded cardiorespiratory parameters (HR and RR) underwent rapid changes in the first hour of anesthesia but stabilized thereafter (Fig. 2b). The observed changes agree with medetomidine pharmacology and with previous rat fMRI studies[20,23,38]. The decrease in HR immediately after medetomidine injection can be attributed to its well-described α_2-adrenergic effects. The activation of central nervous system α_2-adrenoreceptors causes bradycardia due to a decrease in central sympathetic tone, while α_2-adrenoreceptors in the peripheral vasculature mediate vasoconstriction. The latter mechanism leads to a transient elevation in blood pressure, which in turn exacerbates the bradycardia through a baroreceptor-mediated reflex[20]. The respiratory effects of medetomidine alone are considered to be minor[38]. However, medetomidine enhances the potency of isoflurane, and can thus amplify isoflurane-induced respiratory depression[20,39]. This is the most likely explanation for the observed sharp drop in RR right after medetomidine injection, as well as for its gradual recovery following isoflurane discontinuation. This effect necessitates the careful monitoring of animal physiology, especially in the transition period between isoflurane and medetomidine. In order to avoid severe respiratory depression, the speed with which isoflurane is faded out needs to be adapted to each individual animal.

The EFS-evoked activation of the contralateral S1FL (Fig. 3) is described by numerous other rat fMRI studies using the same stimulus[23–25]. For a subset of trials, these studies have also reported activations in the secondary somatosensory area and in sensory thalamic nuclei. If we increase statistical power by grouping multiple fMRI runs in a second-level analysis, we also find the same areas being responsive to EFS (see Supplementary Fig. S8). The shape of the EFS-evoked BOLD response in the S1FL (sharp peak at about 3 s after the onset of stimulation, followed by a plateau sustained till the end of EFS period; see Fig. 3c) is consistent with previous rat fMRI studies[24,40], and the time-to-peak is close to the one reported in rats anesthetized with α-chloralose (2.49 ± 0.31 s)[41]. It is worth noting that this is considerably shorter than the 4–8 s delay commonly assumed in modelling the human hemodynamic response, which could be attributed to a species difference in vascular anatomy and dynamics[41].

The temporal evolution of stimulus-evoked responses exhibited an interesting dependence on the medetomidine administration protocol (Fig. 4). All four protocols converged to steady-state peak ΔBOLD of 2–3% after the first two hours of medetomidine administration, but arrived there through different temporal trajectories. An IV bolus of 0.05 mg/kg followed by a continuous infusion of 0.1 mg/kg/h (protocol 2) had already achieved the steady-state since the early time-window. Deviating from the above dosage, either by omitting the bolus (protocol 3) or by downscaling both bolus and infusion doses (protocol 4), resulted in a time-dependent decrease from the early to the middle time-windows. This implies that early responses under protocols 3 and 4 were stronger than under protocol 2—an effect that appears in the data (Fig. 4c) but does not survive the multiple comparisons correction (see Supplementary Table S11). Omitting the bolus (protocol 3) also led to a time-dependent decrease in global RSFC: the overall pair-wise correlation strength dropped significantly between the early and middle time-windows. This time-dependent attenuation of BOLD readouts in sessions that lacked the bolus could reflect a negative relationship between the strength of these readouts and the concentration of medetomidine. Drug levels in the central nervous system might take hours to stabilize under the continuous infusion regime, given that the pharmacokinetics of medetomidine is characterized by a long terminal half-life of about 57 min, and a hysteresis between plasma and cerebrospinal fluid concentrations[38,42]. Bolus administration likely mediates a faster wash-in of the drug and an earlier establishment of the steady state. For this interpretation, we need to accept that medetomidine dose-dependently suppresses stimulus-evoked BOLD responses and RSFC, at least up to a certain level. Previous studies have in fact found such a dose-dependency for RSFC, but not for stimulus-evoked responses[40,43]. That said, the relevant experiments were restricted to a higher infusion rate range of 0.1–0.3 mg/kg/h (always preceded by a bolus), within which any effects on stimulus-evoked responses could have been saturated.

The case of protocol 1—the SC variant of protocol 2 and the most widely used administration scheme (see Supplementary Table 1)—is a peculiar one. Like protocols 3 and 4, it also exhibited a decrease in peak BOLD between the early and middle time-windows. However, a closer examination of individual rat trajectories (see Supplementary Fig. S7) reveals that this effect was driven by only two rats with exceptionally strong responses within the first 90 minutes; the other four rats produced temporally stable responses. This observation can be interpreted within the framework of dose-dependent response attenuation that was proposed above. Small variations in the injection site and/or the skin temperature may have delayed the drug's absorption into the blood-stream, leading to the observed stronger responses in a sub-set of rats. However, this interpretation cannot be verified without measuring blood concentrations of medetomidine, which we have not performed.

At this point, we would like to emphasize several limitations of the present study. We have no way of dissecting the vascular and neuronal contributions to the observed effects on BOLD readouts: we lack electrophysiological recordings of neural activity and important measures of vascular physiology, such as cerebral blood flow and arterial blood gas concentrations. We also lack fMRI data for very early time points: the earliest fMRI runs

were acquired 30–50 minutes after the onset of medetomidine administration, due to the time spent for animal positioning, structural image acquisition and shimming, and the required overlap between medetomidine administration and isoflurane anesthesia. This delay was most pronounced for protocol 3, during which the said overlap was necessarily prolonged. To put our results into proper context, we would also like to point out the main methodological differences between our study and the existing rat fMRI literature. We used female rats, contrary to almost all other similar studies (Supplementary Table S1). Sex can affect drug metabolism through multiple potential mechanisms[44], so the optimal dosing scheme may differ between males and females. Moreover, the rats in our study were lying supinely in the custom-built rat bed (Supplementary Fig. S2), as opposed to the conventional prone position. In our experience, the supine position reduces respiration-related head motion, to a degree that allows us to avoid using ear bars (See Supplementary Fig. S6). The unconventional position and the absence of ear bars, which are a potentially painful stimulus, could have influenced physiological parameters and the duration of anesthesia.

Despite these limitations, our study does provide an empirical answer to the question of how BOLD readouts evolve over long-lasting medetomidine anesthesia sessions, allowing us to recommend best practices for fMRI studies in rats. Protocols 1 (SC with bolus) and 2 (IV with bolus), which follow the dosage of the originally published protocol[23], are both well-suited for long-lasting fMRI sessions. The choice between them depends on the priorities of the researchers. Whenever maximizing the duration of the steady-state is deemed crucial, protocol 2 is the optimal choice. The main advantage of this protocol lies within the early two hours of anesthesia, since all four protocols converge to a similar steady-state after this time. This is however an important benefit: because the probability of spontaneous wake-ups increases over time, an earlier establishment of the steady-state can significantly prolong the useful experimental time. That said, we recommend always allowing a waiting period of 60 minutes between the bolus injection and the start of functional experiments. The first hour is characterized by rapid changes in cardio-respiratory physiology and is thus best reserved for structural image acquisition. If researchers prefer the practicality of the SC route, they should consider extending this waiting period to 90–120 minutes. We do not claim that these protocols (1 and 2) are necessarily the best choice for rat fMRI, since our study did not include all existing (see Supplementary Table S1) or possible administration protocols. It is however reasonable to consider them as the current 'default' choice, in light of the wealth of available data, and in the interest of promoting comparability among studies.

Methods

Experimental animals.
All experiments followed the standards of the German Federal Law on Care and Use of Laboratory Animals and were approved by the local government authorities (Lower Saxony State Office for Consumer Protection and Food Safety, approval number 33.19-42502-04-15/2042). A total number of 24 female adult Wistar rats (Charles Rivers Laboratories, Sulzfeld Germany) with a median body weight of 308 g (interquartile range 285–350 g) were used for this study. Rats were group-housed in cages with environmental enrichment, at a 12/12-hour light/dark cycle, with 20–24 °C temperature and 45–55% humidity. Water and standard chow were provided ad libitum. The 24 rats were split into four equally sized groups, each assigned to a different protocol of medetomidine administration (see Table 1). No animal was excluded from the experiments or from the analysis. The investigators were not blind to the group allocation.

Anesthesia and monitoring.
Each animal was anesthetized on two sessions separated by a minimum of two weeks. The first session took place on a laboratory bench-top to accommodate unrestricted access to the animal and close monitoring of anesthesia duration and cardio-respiratory physiology (bench session). The functional imaging took place during the second session, performed inside a dedicated small animal MR system (fMRI session). All applied anesthetic protocols followed the same general outline, with isoflurane being used during preparation, and medetomidine during data acquisition (Fig. 1a).

Unconsciousness was induced in a chamber filled with 5% isoflurane and maintained throughout preparation with 2–3% isoflurane in medical air, supplied through a nose cone. The animal was placed in a supine position for both bench and fMRI sessions. The eyes were covered with ophthalmic ointment to prevent them from drying. A cannula was inserted in the SC tissue of the left flank (protocol 1) or in a tail vein (protocols 2–4). Two subdermal needle electrodes were placed in the right forepaw, between the 2nd and the 4th digit. Monitoring equipment was attached, consisting of a rectal temperature probe, a pneumatic pressure sensor placed on the chest, and three SC needle electrodes for electrocardiogram (ECG). After fixing the equipment with adhesive tape, the animal was transferred to a custom-built MRI-compatible rat bed.

Four different protocols of medetomidine administration were used: 1) SC with bolus; 2) IV with bolus; 3) IV no bolus; 4) IV lower dose. The detailed dosing for all protocols is given in Table 1. For protocols 1, 2, and 4, medetomidine (Dorbene vet, Zoetis Deutschland GmbH, Germany) was initially given as a bolus loading dose, followed by a gradual reduction of isoflurane and its eventual discontinuation 10 min later. To mitigate the risk of respiratory depression during this transition period, we tailored the speed of the gradual isoflurane reduction to each individual animal—aiming for a RR range of 40–70 bpm. Continuous infusion of medetomidine commenced 15 min after the bolus. The bolus was omitted for protocol 3, with continuous infusion starting directly after the preparation phase, and isoflurane being gradually reduced to zero over the course of 20–25 min. Attempts to shut off isoflurane earlier led to fast breathing, indicative of an imminent wake-up (bench sessions). All doses were delivered using an MRI-compatible infusion pump (PHD 2000 Infuse/Withdraw; Harvard apparatus, Holliston, Massachusetts, USA), which was loaded with the medetomidine solution diluted 1/20 in saline (final concentration of 0.05 mg/ml). From the start of medetomidine administration, heart rate (HR), respiratory rate (RR), and rectal temperature were monitored using the MR-compatible Model 1030 monitoring and gating system (Small Animal Instruments Inc., Stony Brook, NY 11790, USA). Rectal temperature was kept at 36.5 ± 1 °C using a pad heated by circulating water. Anesthesia was maintained for six hours since the start of

medetomidine administration, except for sessions in which the rat spontaneously woke up earlier. For bench sessions, such wake-ups were identified as spontaneous movements of the rat and were found to be always preceded by the RR getting progressively faster and irregular. Since the animal is not visible during fMRI, the endpoint for fMRI sessions was set based on respiration (RR > 90/min, irregular, and continuously rising for at least 2 min). Anesthesia duration was defined as the time from the start of medetomidine administration (time = 0) till one of the aforementioned endpoints: spontaneous movement, rapid rise in RR, or passage of six hours. Upon reaching an endpoint, the animal was provided with 2% isoflurane through the nose cone and was disconnected from all electrodes, cannulas, and monitoring equipment. Finally, isoflurane was shut off and atipamezole (Atipazole, Prodivet pharmaceuticals, Belgium) was injected SC (0.25 mg/kg for protocols 1–3; 0.175 mg/kg for protocol 4) to facilitate a smooth wake-up.

The monitoring data (HR and RR traces) were recorded at a temporal resolution of 1 s and further processed with in-house python scripts as follows. Firstly, physiologically implausible values—corresponding to data acquisition errors—were dropped. Secondly, fMRI acquisition periods were removed from HR traces, since the rapidly switching magnetic gradients had introduced electrical noise in the ECG recording. Lastly, the traces were smoothed with an exponentially weighted moving average filter (smoothing factor $\alpha = 0.02$). The processed HR and RR traces from bench and fMRI sessions closely resembled each other and were therefore pooled together. For each of the four medetomidine protocols the mean ($\pm$ s.d.) HR/RR trace was calculated across all anesthesia sessions.

MRI acquisition. The fMRI sessions were performed inside a 9.4 Tesla Bruker BioSpec MR system, equipped with the BGA12 gradient, and operated via ParaVision 6.0.1 software. Signal was transmitted via a volume resonator (inner diameter 86 mm) and received by a rat brain 4-channel coil array (all equipment and software from Bruker BioSpin MRI GmbH, Ettlingen, Germany). Approximately 10 min after the discontinuation of isoflurane, the rat was positioned in the isocenter of the MR system, with its body lying supinely and its head fixed with the help of a bite bar. After obtaining low-resolution images for animal localization, a T2-weighted structural image was acquired using a TurboRARE sequence (repetition time 5.225 s, effective echo time 33 ms; 2 averages; RARE factor 8; 30–50 axial slices with a thickness of 0.5 mm; in-plane resolution 0.137×0.137 mm^2; matrix size 256×256). A field map was measured, and shims were adjusted to ensure homogeneity in an ellipsoidal volume encompassing the rat brain (MAPSHIM). This was followed by multiple 330-second-long BOLD fMRI runs, repeated approximately every 10 min, until the experimental endpoint was reached. All fMRI runs were acquired with a single-shot gradient-echo echo planar imaging sequence (220 repetitions; repetition time 1.5 s; echo time 15 ms; flip angle 90°; 30 axial slices with a thickness of 0.5 mm, ascending interleaved slice order with no slice gap; in-plane resolution 0.2×0.2 mm^2; matrix size 128×96; 4 dummy scans; bandwidth 375 kHz). The fMRI slices covered the entire rat brain, excluding the olfactory bulbs and the caudal 3/4 of the cerebellum. Consecutive fMRI runs were alternated between somatosensory fMRI with electrical forepaw stimulation (EFS-fMRI) and resting state fMRI (RS-fMRI) with no stimulus (Fig. 1b). This resulted in a total number of 283 EFS-fMRI and 295 RS-fMRI runs across all rats, spanning from 0.5 up to 6 hours since the start of medetomidine administration. EFS-fMRI runs included a baseline period of 60 s, followed by stimulation of the right forepaw in three 30 s blocks—each paired with 60 s of rest (Fig. 1c). Each stimulus block comprised square unipolar pulses with 3 mA amplitude and 0.3 ms pulse width, delivered at 9 Hz (Stimulus Generator 4002, Multi Channel Systems MCS GmbH, Reutlingen, Germany). The above parameters were chosen based on previous EFS studies in medetomidine-anesthetized rats[24,25,45].

MRI preprocessing. All MR images were first exported from ParaVision to DICOM format and then converted to NIfTI (Neuroimaging Informatics Technology Initiative; http://nifti.nimh.nih.gov) using the dcm2nii (https://www.nitrc.org/projects/dcm2nii/) tool. The structural T2-weighted images were used to construct a study template with the help of the Advanced Normalization Tools software—ANTs (http://stnava.github.io/ANTs/). The structural image of one of the rats was chosen as the target reference space. Every other structural image was registered to the target in two steps. First a linear rigid (3 translations and 3 rotations) registration was used to bring each structural image to the same origin and orientation as the reference image. This was followed by a non-linear symmetric diffeomorphic (SyN) registration to account for differences in brain size and shape[46]. All 24 structural images were averaged in the reference space to produce a mean anatomical image. A down-sampled ($0.2 \times 0.2 \times 0.5$ mm^3) version of this image was used to create a brain mask and served as the study template to which all functional datasets were eventually registered. The fMRI image series were preprocessed using functions from multiple neuroimaging toolkits, combined into a pipeline with python's Nipype library[47]. Images were corrected for slice timing with FSL (FMRIB Software Library, https://fsl.fmrib.ox.ac.uk/fsl/fslwiki/) and temporally filtered with AFNI (https://afni.nimh.nih.gov/). A high-pass filter of 0.01 Hz was used to remove slow temporal drifts, with an additional low-pass filter of 0.15 Hz being applied to RS-fMRI datasets only. Spatial smoothing (FSL) was performed using a 0.5 mm 3D Gaussian kernel. We chose to skip motion correction and regression of nuisance variables, as these preprocessing steps were shown to have little effect in anesthetized and head-fixed rodents[48]. Besides, a quantification of motion parameters showed that motion was minimal across all fMRI runs (see Supplementary Fig. S6). A rigid transformation matrix was calculated between the mean image of each functional run and the native structural image. This matrix was combined with the previously calculated linear and non-linear transforms into a composite warp file, which was used to transform the preprocessed fMRI datasets into the study template space (ANTs).

fMRI analysis and statistics. Areas activated during each EFS-fMRI run were identified via a first-level general linear model analysis carried out using FEAT (FMRI Expert Analysis Tool) Version 6.00, part of FSL[49].

The stimulus time course (1 during stimulation, 0 elsewhere) was convolved with a standard double-gamma hemodynamic response function to generate the model predictor. The resulting statistical maps were masked for brain, thresholded non-parametrically using clusters determined by z > 3.1 and a corrected cluster significance threshold of p = 0.05[50,51], binarized, and averaged across all 283 EFS-fMRI runs to construct an overall activation probability map. The region active in at least 30% of all EFS-fMRI runs (contralateral S1FL; see Fig. 3a) was taken as a region-of-interest (ROI). This ROI's mean BOLD time course was extracted from each EFS-fMRI run, normalized to the pre-stimulus baseline, and averaged across the three stimulation blocks to produce an event-related average. The peak % signal change (peak ΔBOLD) was extracted from the event-related average, as a measure of BOLD response strength (Fig. 3b). We also performed a second-level fixed-effects analysis (FEAT) for each medetomidine protocol, by pooling the corresponding EFS-fMRI runs and computing the mean group effect. The resulting statistical maps were masked for brain and thresholded non-parametrically using maximum height thresholding based on Gaussian random field theory, with a (corrected) significance threshold of P = 0.05[50,51].

Resting state functional connectivity (RSFC) analysis was performed using in-house python scripts. All 295 preprocessed RS-fMRI datasets were normalized by subtracting the temporal mean and dividing by the standard deviation. Normalized BOLD signal time courses were extracted from 28 ROIs (14 on each hemisphere), manually delineated based on the Paxinos-Watson rat brain atlas[52] (see Fig. 5a, left). Pearson's correlation coefficients were calculated for all ROI pairs, transformed into Fisher's Z-scores, and stored as a pair-wise correlation matrix. The mean Z-score across all 378 unique ROI pairs served as a measure of global RSFC. To visualize the hierarchical structure of the functional connectome, each correlation matrix was also represented as a weighted graph, with the ROIs as nodes and the ROI pairs as edges. The edges were ranked by ascending correlation strength, and the rank was assigned as the numerical weight of the edge (strongest correlation to highest weight). Figure 5a (right) depicts a pair-wise correlation matrix and its graph representation for an example RS-fMRI run.

Statistical analysis was performed in R, version 3.6.1 (https://www.r-project.org/). We used the lmer function of the lme4 package[53] to design a linear mixed effects model, separately for each of two response variables: the EFS-evoked response strength (peak ΔBOLD) and the global RSFC (mean Z-score). This model can account for the repeated-measures design of the study and for missing data points (e.g. due to spontaneous earlier wake-ups). The fMRI runs were grouped into three two-hour-long time-windows (early: 0–2 h; middle: 2–4 h; late: 4–6 h), based on the onset time of their acquisition. The time-window, the medetomidine administration protocol, and their interaction were modeled as fixed effects, while individual rat intercepts were included as random effects. This approach treats the time-window as a within-subject repeated-measures factor and the medetomidine protocol as a between-subject factor. Model inference and statistical tests were carried out using the lmerTest package[54]. Specifically, Satterthwaite's method was used to create Type III Analysis of Variance (ANOVA) tables, and the ls_means function was used to estimate Least Squares Means for all sub-classes (levels of protocol, time-window, and their combinations). Finally, the difflsmeans function was applied to estimate pair-wise differences between the sub-class means; the resulting p-values were adjusted for multiple comparisons according to the Holm method[55]. The ANOVA tables and the outputs of ls_means and difflsmeans functions can be found in the Supplementary Material (Supplementary Tables S9–S12).

Data availability

The unprocessed anatomical and functional MRI data are publicly available through the OpenNeuro repository (https://openneuro.org/datasets/ds001981/). They are provided in NIfTI format and organized according to the BIDS specification (Brain Imaging Data Structure, https://bids.neuroimaging.io/). The preprocessing scripts (python) can be shared upon request.

References

1. Ogawa, S., Lee, T. M., Kay, A. R. & Tank, D. W. Brain magnetic resonance imaging with contrast dependent on blood oxygenation. *Proc. Natl. Acad. Sci.* **87**, 9868–9872 (1990).
2. Biswal, B., Zerrin Yetkin, F., Haughton, V. M. & Hyde, J. S. Functional connectivity in the motor cortex of resting human brain using echo-planar mri. *Magn. Reson. Med.* **34**, 537–541 (1995).
3. Fox, M. D. & Raichle, M. E. Spontaneous fluctuations in brain activity observed with functional magnetic resonance imaging. *Nat. Rev. Neurosci.* **8**, 700–711 (2007).
4. Greicius, M. Resting-state functional connectivity in neuropsychiatric disorders. *Curr. Opin. Neurol.* **24**, 424–430 (2008).
5. Jonckers, E., Shah, D., Hamaide, J., Verhoye, M. & van der Linden, A. The power of using functional fMRI on small rodents to study brain pharmacology and disease. *Front. Pharmacol.* **6**, 231 (2015).
6. Albers, F., Wachsmuth, L., van Alst, T. M. & Faber, C. Multimodal Functional Neuroimaging by Simultaneous BOLD fMRI and Fiber-Optic Calcium Recordings and Optogenetic Control. *Mol. Imaging Biol.* **20**, 171–182 (2018).
7. Schulz, K. *et al.* Simultaneous BOLD fMRI and fiber-optic calcium recording in rat neocortex. *Nat. Methods* **9**, 597–602 (2012).
8. Yu, X. *et al.* Sensory and optogenetically driven single-vessel fMRI. *Nat. Methods* **13**, 337 EP- (2016).
9. Wang, M., He, Y., Sejnowski, T. J. & Yu, X. Brain-state dependent astrocytic Ca^{2+} signals are coupled to both positive and negative BOLD-fMRI signals. *Proc. Natl. Acad. Sci. USA* **115**, E1647–E1656 (2018).
10. Gao, Y. R. *et al.* Time to wake up: Studying neurovascular coupling and brain-wide circuit function in the un-anesthetized animal. *Neuroimage* **153**, 382–398 (2017).
11. Liang, Z., Liu, X. & Zhang, N. Dynamic resting state functional connectivity in awake and anesthetized rodents. *Neuroimage* **104**, 89–99 (2015).
12. Paasonen, J., Stenroos, P., Salo, R. A., Kiviniemi, V. & Gröhn, O. Functional connectivity under six anesthesia protocols and the awake condition in rat brain. *Neuroimage* **172**, 9–20 (2018).
13. Masamoto, K. & Kanno, I. Anesthesia and the quantitative evaluation of neurovascular coupling. *J. Cereb. Blood Flow Metab.* **32**, 1233–1247 (2012).

14. Pan, W.-J., Billings, J. C. W., Grooms, J. K., Shakil, S. & Keilholz, S. D. Considerations for resting state functional MRI and functional connectivity studies in rodents. *Front. Neurosci.* **9**, 269 (2015).
15. Schroeter, A., Schlegel, F., Seuwen, A., Grandjean, J. & Rudin, M. Specificity of stimulus-evoked fMRI responses in the mouse: the influence of systemic physiological changes associated with innocuous stimulation under four different anesthetics. *Neuroimage* **94**, 372–384 (2014).
16. Grandjean, J., Schroeter, A., Batata, I. & Rudin, M. Optimization of anesthesia protocol for resting-state fMRI in mice based on differential effects of anesthetics on functional connectivity patterns. *Neuroimage* **102**(Pt 2), 838–847 (2014).
17. Schlegel, F., Schroeter, A. & Rudin, M. The hemodynamic response to somatosensory stimulation in mice depends on the anesthetic used: Implications on analysis of mouse fMRI data. *Neuroimage* **116**, 40–49 (2015).
18. Shim, H.-J. *et al.* Mouse fMRI under ketamine and xylazine anesthesia: Robust contralateral somatosensory cortex activation in response to forepaw stimulation. *Neuroimage* **177**, 30–44 (2018).
19. Scheinin, H., Virtanen, R., Macdonald, E., Lammintausta, R. & Scheinin, M. Medetomidine — a novel α2-adrenoceptor agonist: A review of its pharmacodynamic effects. *Prog. Neuro-Psychopharmacology Biol. Psychiatry* **13**, 635–651 (1989).
20. Sinclair, M. D. A review of the physiological effects of alpha2-agonists related to the clinical use of medetomidine in small animal practice. *Can. Vet. J.* **44**, 885–897 (2003).
21. Brown, E. N., Purdon, P. L. & van Dort, C. J. General anesthesia and altered states of arousal: a systems neuroscience analysis. *Annu. Rev. Neurosci.* **34**, 601–628 (2011).
22. Weber, R., Ramos-Cabrer, P., Wiedermann, D. & Hoehn, M. A longitudinal and totally noninvasive fMRI protocol in rats. *J. Cereb. Blood Flow Metab.* **25**, S361–S361 (2005).
23. Weber, R., Ramos-Cabrer, P., Wiedermann, D., Van Camp, N. & Hoehn, M. A fully noninvasive and robust experimental protocol for longitudinal fMRI studies in the rat. *Neuroimage* **29**, 1303–1310 (2006).
24. Zhao, F., Zhao, T., Zhou, L., Wu, Q. & Hu, X. BOLD study of stimulation-induced neural activity and resting-state connectivity in medetomidine-sedated rat. *Neuroimage* **39**, 248–260 (2008).
25. Pawela, C. P. *et al.* A protocol for use of medetomidine anesthesia in rats for extended studies using task-induced BOLD contrast and resting-state functional connectivity. *Neuroimage* **46**, 1137–1147 (2009).
26. Williams, K. A. *et al.* Comparison of alpha-chloralose, medetomidine and isoflurane anesthesia for functional connectivity mapping in the rat. *Magn. Reson. Imaging* **28**, 995–1003 (2010).
27. Kalthoff, D., Po, C., Wiedermann, D. & Hoehn, M. Reliability and spatial specificity of rat brain sensorimotor functional connectivity networks are superior under sedation compared with general anesthesia. *NMR Biomed.* **26**, 638–650 (2013).
28. Boretius, S., Tammer, R., Michaelis, T., Brockmoller, J. & Frahm, J. Halogenated volatile anesthetics alter brain metabolism as revealed by proton magnetic resonance spectroscopy of mice *in vivo*. *Neuroimage* **69**, 244–255 (2013).
29. Masamoto, K., Kim, T., Fukuda, M., Wang, P. & Kim, S.-G. Relationship between neural, vascular, and BOLD signals in isoflurane-anesthetized rat somatosensory cortex. *Cereb. Cortex* **17**, 942–950 (2007).
30. Pisauro, M. A., Dhruv, N. T., Carandini, M. & Benucci, A. Fast Hemodynamic Responses in the Visual Cortex of the Awake Mouse. *J. Neurosci.* **33**, 18343 LP–18351 (2013).
31. Aksenov, D. P., Li, L., Miller, M. J., Iordanescu, G. & Wyrwicz, A. M. Effects of anesthesia on BOLD signal and neuronal activity in the somatosensory cortex. *J. Cereb. Blood Flow Metab.* **35**, 1819–26 (2015).
32. Liu, X., Zhu, X.-H., Zhang, Y. & Chen, W. The change of functional connectivity specificity in rats under various anesthesia levels and its neural origin. *Brain Topogr.* **26**, 363–377 (2013).
33. Magnuson, M. E., Thompson, G. J., Pan, W. J. & Keilholz, S. D. Time-dependent effects of isoflurane and dexmedetomidine on functional connectivity, spectral characteristics, and spatial distribution of spontaneous BOLD fluctuations. *NMR Biomed.* **27**, 291–303 (2014).
34. Chuang, K.-H. & Nasrallah, F. A. Functional networks and network perturbations in rodents. *Neuroimage* **163**, 419–436 (2017).
35. Brynildsen, J. K. *et al.* Physiological characterization of a robust survival rodent fMRI method. *Magn. Reson. Imaging* **35**, 54–60 (2017).
36. Fukuda, M., Vazquez, A. L., Zong, X. & Kim, S.-G. G. Effects of the alpha(2)-adrenergic receptor agonist dexmedetomidine on neural, vascular and BOLD fMRI responses in the somatosensory cortex. *Eur. J. Neurosci.* **37**, 80–95 (2013).
37. van Alst, T. M. *et al.* Anesthesia differentially modulates neuronal and vascular contributions to the BOLD signal. *Neuroimage* **195**, 89–103 (2019).
38. Bol, C. J. J. G., Danhof, M., Stanski, D. R. & Mandema, J. W. Pharmacokinetic-Pharmacodynamic Characterization of the Cardiovascular, Hypnotic, EEG and Ventilatory Responses to Dexmedetomidine in the Rat. *J. Pharmacol. Exp. Ther.* **283**, 1051–1058 (1997).
39. Ewing, K. K., Mohammed, H. O., Scarlett, J. M. & Short, C. E. Reduction of isoflurane anesthetic requirement by medetomidine and its restoration by atipamezole in dogs. *Am. J. Vet. Res.* **54**, 294–9 (1993).
40. Nasrallah, F. A., Lew, S. K., Low, A. S.-M. & Chuang, K.-H. Neural correlate of resting-state functional connectivity under α2 adrenergic receptor agonist, medetomidine. *Neuroimage* **84**, 27–34 (2014).
41. Silva, A. C., Koretsky, A. P. & Duyn, J. H. Functional MRI impulse response for BOLD and CBV contrast in rat somatosensory cortex. *Magn. Reson. Med.* **57**, 1110–1118 (2007).
42. Bol, C. J. J. G., Vogelaar, J. P. W. & Mandema, J. W. Anesthetic profile of dexmedetomidine identified by stimulus-response and continuous measurements in rats. *J. Pharmacol. Exp. Ther.* **291**, 153–60 (1999).
43. Nasrallah, F. A., Tan, J. & Chuang, K.-H. H. Pharmacological modulation of functional connectivity: α2-adrenergic receptor agonist alters synchrony but not neural activation. *Neuroimage* **60**, 436–446 (2012).
44. Czerniak, R. Gender-Based Differences in Pharmacokinetics in Laboratory Animal Models. *Int. J. Toxicol.* **20**, 161–163 (2001).
45. Li, N., Van Zijl, P., Thakor, N. & Pelled, G. Study of the spatial correlation between neuronal activity and BOLD fMRI responses evoked by sensory and channelrhodopsin-2 stimulation in the rat somatosensory cortex. *J. Mol. Neurosci.* **53**, 553–561 (2014).
46. Avants, B. B., Epstein, C. L., Gossman, M. & Gee, J. C. Symmetric diffeomorphic image registration with cross-correlation: Evaluating automated labeling of elderly and neurodegenerative brain. *Med. Image Anal.* **12**, 26–41 (2008).
47. Gorgolewski, K. *et al.* Nipype: A Flexible, Lightweight and Extensible Neuroimaging Data Processing Framework in Python. *Front. Neuroinform.* **5**, 13 (2011).
48. Chuang, K. H. *et al.* Evaluation of nuisance removal for functional MRI of rodent brain. *Neuroimage* **188**, 694–709 (2019).
49. Woolrich, M. W., Ripley, B. D., Brady, M. & Smith, S. M. Temporal Autocorrelation in Univariate Linear Modeling of FMRI Data. *Neuroimage* **14**, 1370–1386 (2001).
50. Smith, S. M. Overview of fMRI analysis. in *Functional Magnetic Resonance Imaging* 216–230 (Oxford University Press, 2001).
51. Worsley, K. J. Statistical analysis of activation images. in *Functional Magnetic Resonance Imaging* 251–270 (Oxford University Press, 2001).
52. Paxinos, G. & Watson, C. *The rat brain in stereotaxic coordinates*. (Elsevier, 2007).
53. Bates, D., Mächler, M., Bolker, B. & Walker, S. Fitting Linear Mixed-Effects Models Using lme4. *J. Stat. Softw.* **67**, 1–48 (2015).
54. Kuznetsova, A., Brockhoff, P. & Christensen, R. lmerTest Package: Tests in Linear Mixed Effects Models. *J. Stat. Software, Artic.* **82**, 1–26 (2017).
55. Holm, S. A Simple Sequentially Rejective Multiple Test Procedure. *Scand. J. Stat.* **6**, 65–70 (1979).

Acknowledgements

Author contributions

The study was devised by J.B. and S.B. Experiments and data analysis were performed by N.S. Results were discussed and interpreted by all co-authors. The manuscript was written by N.S., in consultation with S.B. and J.B. All authors reviewed the manuscript.

Competing interests

The authors declare no competing interests.

Additional information

Supplementary information is available for this paper at https://doi.org/10.1038/s41598-019-53144-y.

Correspondence and requests for materials should be addressed to N.S.

Reprints and permissions information is available at www.nature.com/reprints.

Publisher's note Springer Nature remains neutral with regard to jurisdictional claims in published maps and institutional affiliations.